THE JOURNAL OF BIOLOGICAL CHEMISTRY VOL. 287, NO. 16, pp. 13216–13227, April 13, 2012
Published in the U.S.A.

Myocilin Interacts with Syntrophins and Is Member of Dystrophin-associated Protein Complex*[S]

Received for publication, January 21, 2012, and in revised form, February 23, 2012 Published, JBC Papers in Press, February 25, 2012, DOI 10.1074/jbc.M111.224063

Myung Kuk Joe[‡], Changwon Kee[§], and Stanislav I. Tomarev[‡1]

From the [‡]Retinal Ganglion Cell Biology Section, Laboratory of Retinal Cell and Molecular Biology, NEI, National Institutes of Health, Bethesda, Maryland 20892 and the [§]Department of Ophthalmology, Samsung Medical Center, Sungkyunkwan University School of Medicine, Seoul 135-710, Korea

Background: The non-ocular function(s) of myocilin, a glaucoma-associated protein, is not known.
Results: Myocilin interacts with syntrophin, a component of dystrophin-associated protein complex (DAPC) and increases phosphorylation of several regulators of muscle size.
Conclusion: Myocilin is involved in the muscle hypertrophy pathways acting through the components of DAPC.
Significance: This is the first demonstration of myocilin functions in the skeletal muscles.

Genetic studies have linked myocilin to open angle glaucoma, but the functions of the protein in the eye and other tissues have remained elusive. The purpose of this investigation was to elucidate myocilin function(s). We identified α1-syntrophin, a component of the dystrophin-associated protein complex (DAPC), as a myocilin-binding candidate. Myocilin interacted with α1-syntrophin via its N-terminal domain and co-immunoprecipitated with α1-syntrophin from C2C12 myotubes and mouse skeletal muscle. Expression of 15-fold higher levels of myocilin in the muscles of transgenic mice led to the elevated association of α1-syntrophin, neuronal nitric-oxide synthase, and α-dystroglycan with DAPC, which increased the binding of laminin to α-dystroglycan and Akt signaling. Phosphorylation of Akt and Forkhead box O-class 3, key regulators of muscle size, was increased more than 3-fold, whereas the expression of muscle-specific RING finger protein-1 and atrogin-1, muscle atrophy markers, was decreased by 79 and 88%, respectively, in the muscles of transgenic mice. Consequently, the average size of muscle fibers of the transgenic mice was increased by 36% relative to controls. We suggest that intracellular myocilin plays a role as a regulator of muscle hypertrophy pathways, acting through the components of DAPC.

Myocilin was identified in a human trabecular meshwork cell line as a glucocorticoid-induced protein more than 10 years ago (1). Subsequent experiments demonstrated that myocilin belongs to a family of olfactomedin domain-containing proteins that consists of 13 members in mammals (2). Most of the olfactomedin domain-containing proteins, including myocilin, are secreted glycoproteins that demonstrate specific expression patterns. The N-terminal region of myocilin contains a leucine zipper, which is part of two coiled-coil domains, whereas the C-terminal region contains the olfactomedin domain. Myocilin is able to form dimers and multimers, and the N-terminal region of myocilin is critical for dimerization (3–6).

It is now well established that mutations in the myocilin (*MYOC*) gene may lead to glaucoma and are found in more than 10% of juvenile open angle glaucoma cases and in 3–4% of patients with adult onset primary open angle glaucoma (7–10). Glaucoma is one of the leading causes of irreversible blindness in the world. It is estimated to affect more than 60 million and blind about 4.5 million people worldwide (11). Primary open angle glaucoma is the most common form of glaucoma. More than 70 glaucoma-causing mutations in the *MYOC* gene have been identified, and greater than 90% of them are located in the region encoding the olfactomedin domain. Mutations causing a severe glaucoma phenotype lead to the retention of myocilin in the endoplasmic reticulum and prevent its secretion. Moreover, secretion of wild-type myocilin is impeded in the presence of mutated myocilin protein (12–15). Accumulation of mutated myocilin in the endoplasmic reticulum may be deleterious for cells, making them more sensitive to oxidative stress leading to cell death (16–18).

The *MYOC* gene is highly expressed in the trabecular meshwork, iris, ciliary body, sclera, and retinal pigmented epithelial cells, with lower levels of expression observed in skeletal muscle, mammary gland, thymus, and testis (5, 8, 10, 19). Available data suggest that the presence of wild-type myocilin is not critical for normal development and survival. Mice heterozygous and homozygous for a targeted null mutation in myocilin do not have a detectable phenotype (20). Similarly, it has been reported that an elderly woman homozygous for the Arg46Stop mutation in the *MYOC* gene do not develop identifiable pathologies (21).

The functions of wild-type myocilin are still not very clear. One approach to the elucidation of protein functions includes the identification of proteins interacting with the protein of interest or the identification of protein complexes containing the protein of interest. Recently, we demonstrated that myocilin, similar to Wnt proteins, interacts with cysteine-rich domains of several frizzled receptors and secreted frizzled-related proteins as well as with Wnt inhibitory factor WIF-1 (22).

* This work was supported, in whole or in part, by the National Institutes of Health, NEI, Intramural Research Program.
[S] This article contains supplemental Figs. 1–3.
[1] To whom correspondence should be addressed: Retinal Ganglion Cell Biology Section, Laboratory of Retinal Cell and Molecular Biology, National Eye Institute, NIH, Bldg. 6, Rm. 212A, 6 Center Dr., Bethesda, MD 20892. Tel.: 301-496-8524; E-mail: tomarevs@nei.nih.gov.

Myocilin may modify the organization of the actin cytoskeleton, stimulating the formation of stress fibers, and this may be essential for the contractility of the trabecular meshwork and the regulation of intraocular pressure (22). We suggested that myocilin may serve as a modulator of Wnt signaling and that other family members or Wnt proteins may compensate for an absence of myocilin by performing its functions (22).

In the present work, we demonstrate that myocilin is part of the dystrophin-associated protein complex (DAPC)[2] in mouse skeletal muscle and in differentiating C2C12 cells forming myotubes. Myocilin interacts with α1-syntrophin (α1-Syn), a cytoplasmic component of the DAPC, that serves as a scaffolding adapter. Overexpression of myocilin in transgenic mice leads to a redistribution of some DAPC proteins and increased phosphorylation of Akt, mTOR, and Forkhead box O-class 3 (FoxO3) transcription factor, the key regulators of muscle size. Moreover, the muscle size was increased in transgenic mice compared with wild-type mice. We suggest that myocilin is one of the regulators of muscle hypertrophy pathways.

EXPERIMENTAL PROCEDURES

Cell Cultures—Mouse C2C12 myoblasts were cultured in Dulbecco's modified Eagle's medium (DMEM) containing 15% fetal bovine serum, 0.1 mg/ml penicillin, and 0.1 mg/ml streptomycin at 37 °C in a humidified atmosphere with 5% CO_2. When C2C12 myoblasts were grown to 80–90% confluence, the growth medium was replaced with DMEM containing 2% horse serum to induce myotube differentiation. Cells were cultured for 4–5 days with fresh medium exchanged daily until differentiated myotubes were observed.

Antibodies—Rabbit polyclonal antibody against mouse myocilin was described previously (14). Other antibodies were purchased from the following sources: anti-α1-Syn, anti-pan-syntrophin (1351), and anti-laminin from Abcam (Cambridge, MA); anti-FoxO3a from Sigma; anti-heat shock cognate 70 (HSC70) and anti-β-dystroglycan (β-DG) from Santa Cruz Biotechnology, Inc. (Santa Cruz, CA); anti-phospho-FoxO3a and anti-α-dystroglycan (α-DG, IIH6) from Millipore (Bedford, MA); anti-α-dystrobrevin, anti-neuronal nitric-oxide synthase (nNOS), and anti-protein-disulfide isomerase from BD Transduction Laboratories (San Diego, CA); anti-AKT1, anti-phospho-AKT1, anti-mTOR, anti-phospho-mTOR, and anti-phospho-p70 S6 kinase from Cell Signaling (Beverly, MA); anti-dystrophin from Vector Laboratories (Burlingame, CA); anti-myosin heavy chain from R&D Systems (Minneapolis, MN); and anti-pigment epithelium-derived factor from Bio-Products MD (Middletown, MD). Anti-pan-syntrophin was labeled with HRP using the SureLINK HRP conjugation kit (KPL, Gaithersburg, MD), and anti-α1-Syn was labeled with fluorescent dye using the DyLight 594 antibody labeling kit (Pierce) according to the manufacturer's instructions.

Yeast Two-hybrid Assay—A yeast two-hybrid screen was performed according to the manufacturer's instructions for Matchmaker system 3 (Clontech) as described previously (23). To identify the domain on myocilin that is involved in the interaction with α1-Syn, we transformed AH109 cells with pGBKT7-myocilin constructs (positions 33–504, 33–245, and 246–504 in the human myocilin sequence) or the empty pGBKT7 vector. The AH109 cells pretransformed with the above pGBKT7 constructs were mated with Y187 cells pretransformed with the pACT2-α1-Syn at 30 °C in 2× YPD medium. The mated yeasts were spotted onto −LT and −AHLT selective mediums.

Immunoblotting—C2C12 myoblasts and myotubes grown on 12-well plates were dissolved in 1 ml of 1× Laemmli buffer (Invitrogen). Conditioned media were harvested and centrifuged at 1000 × *g* for 10 min, and the cleared supernatants were mixed with the Laemmli buffer. Skeletal muscle samples were weighed and homogenized in 20 volumes of sample treatment buffer (75 mM Tris-Cl, pH 6.8, 15% SDS, 20% glycerol, 6% mercaptoethanol, and 0.001% bromphenol blue) with a Polytron PT 2100 homogenizer (Kinematica AG, Lucerne, Switzerland). The samples were boiled for 5 min and centrifuged at 1000 × *g* for 3 min. Equal amounts of proteins were separated by NuPAGE 4–12% gradient BisTris gel (Invitrogen) and transferred to a nitrocellulose membrane (Invitrogen). Membranes were preincubated in a blocking buffer (5% nonfat milk, 25 mM Tris, pH 7.4, 150 mM NaCl, and 0.05% Tween 20) and then incubated with each antibody in blocking buffer overnight at 4 °C. Secondary antibodies (an anti-rabbit or anti-mouse HRP-conjugated antibody, Amersham Biosciences) were diluted 1:5000 in blocking buffer and incubated for 2 h at room temperature. The immunolabeled protein bands were visualized with SuperSignal WestDura (Pierce). For quantification, scanned images were analyzed by ImageJ software (National Institutes of Health, Bethesda, MD).

Immunoprecipitation—Differentiated C2C12 myotubes were rinsed with phosphate-buffered saline (PBS), scraped off in PBS, and pelleted. The pellets were resuspended in Mg^{2+} lysis buffer (25 mM HEPES, pH 7.5, 150 mM NaCl, 1% Igepal CA-630, 10 mM $MgCl_2$, 1 mM EDTA, and 2% glycerol) containing a protease inhibitor mixture (Roche Applied Science) and homogenized using a Polytron PT 2100 homogenizer (Kinematica AG). Insoluble material was removed by centrifugation, and the protein concentration of the soluble fractions was determined by the Bradford protein assay (Bio-Rad). Equivalent amounts of soluble fractions were incubated with anti-α1-Syn antibody or anti-myocilin antibody for 2 h at 4 °C followed by incubation with 30 μl of protein G-agarose beads (Roche Applied Science) overnight at 4 °C. The bead-antibody complexes were collected by centrifugation, rinsed three times in the lysis buffer, resuspended in 1× Laemmli sample buffer, boiled for 5 min, and subjected to immunoblotting as described above. Mouse skeletal muscles were dissected and homogenized in Mg^{2+} lysis buffer using a Polytron PT 2100 homogenizer (Kinematica AG). Immunoprecipitation was performed as described above for the myotubes. Immunoprecipitation for dystrophin from skeletal muscle tissue was performed using the Cross-link Immunoprecipitation Kit (Pierce) according to the manufacturer's instructions.

[2] The abbreviations used are: DAPC, dystrophin-associated protein complex; α1-Syn, α1-syntrophin; DG, dystroglycan; nNOS, neuronal nitric-oxide synthase; BisTris, 2-[bis(2-hydroxyethyl)amino]-2-(hydroxymethyl)propane-1,3-diol; TA, tibialis anterior; WGA, wheat germ agglutinin; mTOR, mammalian target of rapamycin.

Immunofluorescent Labeling—C2C12 myoblasts were seeded onto collagen I-coated coverslips (BD Biosciences) at 80% confluence. The myoblasts or myotubes were fixed in 4% paraformaldehyde for 10 min. For α1-Syn staining, the coverslips were incubated in antigen retrieval buffer (100 mM Tris, 5% urea, pH 9.5) at 95 °C for 10 min. The fixed samples were permeabilized with 0.5% Tween 20 for 30 min and blocked in a solution of 1% bovine serum albumin (BSA) in PBS for 30 min. The samples were then incubated in a solution of 1% BSA in PBS with the primary antibody at 4 °C for 16 h. The samples were washed twice for 10 min in PBS containing 0.01% Tween 20, followed by incubation with Alexa 594-conjugated anti-rabbit secondary antibody and Alexa 488-conjugated anti-mouse secondary antibody (Molecular Probes, Inc., Eugene, OR) for 30 min. After washing four times with PBS containing 0.01% Tween 20, the samples were mounted in Vectashield mounting medium with DAPI (Vector Laboratories) or further incubated with DyLight 594-labeled anti-α1-Syn antibody for 3 h to stain α1-Syn. Dissected mouse tibialis anterior (TA) muscles were fixed in 4% paraformaldehyde for 30 min. The fixed tissues were soaked in 30% sucrose in PBS at 4 °C overnight, embedded in optimal cutting temperature compound, and quickly frozen with liquid nitrogen. Transverse sections (10 μm thick) were cut with a cryostat (Leica CM 3050, Leica Microsystems, Wetzlar, Germany). The sections were blocked in a solution of 2% NGS and 0.2% Triton X-100 in PBS for 1 h and then incubated with primary antibodies at room temperature for 3 h. Subsequently, the tissues were incubated with Alexa 594-labeled anti-rabbit secondary antibody at room temperature for 1 h. For the double-staining of myocilin and α1-Syn, the sections were additionally incubated with DyLight 594-labeled anti-α1-Syn antibody for 3 h. Fluorescent staining was examined by an Axioplan-2 fluorescence microscope (Carl Zeiss, Jena, Germany) or LSM 700 confocal laser-scanning microscope (Carl Zeiss). To determine individual fiber size in each section, the cross-sectional area was measured by tracing the laminin staining using ImageJ analysis software (National Institutes of Health).

Biochemical Analysis of DAPC Stability—Skeletal muscle tissues were homogenized in 10 volumes of digitonin buffer (50 mM Tris-HCl, pH 7.5, 500 mM NaCl, and 1% digitonin) containing a protease inhibitor mixture (Roche Applied Science). After centrifugation, the soluble fractions were incubated with a wheat germ agglutinin (WGA)-agarose resin (Vector Laboratories) for 2 h at 4 °C. Bound proteins were eluted with 1× Laemmli sample buffer and used for Western blot analysis using antibodies against dystrophin and β-DG. The intensity of each band was quantified using ImageJ analysis software. Relative levels of dystrophin in WGA eluates were normalized relative to β-DG signals.

Laminin Overlay Assay—For the enrichment of α-DG from skeletal muscle, the muscle lysates were prepared in Mg^{2+} lysis buffer as described above for immunoprecipitation and incubated with WGA-agarose resin (Vector Laboratories) for 2 h at 4 °C. The elutes from the WGA-agarose resin were separated by a NuPAGE 4–12% gradient BisTris gel (Invitrogen) and transferred to a nitrocellulose membrane (Invitrogen). To assess laminin binding to α-DG, the nitrocellulose membranes were blocked in laminin binding buffer (10 mM triethanolamine, pH 7.6, 140 mM NaCl, 1 mM $MgCl_2$, 1 mM $CaCl_2$, and 5% nonfat milk) and then were incubated with 1 μg/ml Engelbreth-Holm-Swarm laminin (BD Biosciences) in laminin binding buffer overnight at 4 °C. Bound laminin was detected with polyclonal laminin antibodies (Abcam) by chemiluminescence.

Real-time PCR Analysis—C2C12 myoblasts, myotubes, or skeletal muscle were homogenized in a TRIzol reagent (Invitrogen) using a Polytron PT 2100 homogenizer (Kinematica AG), and total RNA was extracted according to the manufacturer's directions. cDNA was obtained by reverse transcription of mRNA by using a SuperScript III first-strand synthesis system (Invitrogen). Quantitative PCR was carried out on a 7900HT real-time thermocycler (ABI, Foster City, CA) using a SYBR Green PCR master mix (ABI). The primers used were specific for myocilin (forward, 5′-TACCCCTCTCAGGACATGCT; reverse, 5′-GCCAGATGGATTTTCCTTCA), muscle-specific RING finger protein 1 (MuRF-1; forward, 5′-TGAGGTGCCTACTTGCTCCT; reverse, 5′-TCACCTGGTGGCTATTCTCC), atrogin-1 (forward, 5′-ATGCACACTGGTGCAGAGAG; reverse, 5′-TGTAAGCACACAGGCAGGTC), or glyceraldehyde-3-phosphate dehydrogenase (GAPDH; forward, 5′-GTCTCCTGCGACTTCAAC; reverse, 5′-TCATTGTCATACCAGGAAATGAGC). GAPDH was used as an internal control.

Histological Analysis—Excised TA muscles were fixed in 4% paraformaldehyde, embedded in paraffin, and sectioned at 10 μm. The prepared transverse sections were subjected to hematoxylin and eosin (H&E) or Masson trichrome staining, following the standard protocols.

Statistics—Quantitative data are expressed as mean ± S.E. Statistical differences between two groups were determined by two-tailed Student's *t* test using Microsoft Excel 2007 software. Values were considered significantly different if p was <0.05.

RESULTS

Myocilin Expression Is Up-regulated in Differentiating Muscle Cells—Because myocilin is known to be expressed in skeletal muscle (3, 19), we tested whether myocilin is expressed in the mouse myoblast C2C12 cell line. The levels of *Myoc* mRNA and myocilin protein were very low in myoblasts but were dramatically increased in differentiating C2C12 cells forming myotubes (Fig. 1, *A* and *B*). Similarly, myoblasts showed very low myocilin and heavy myosin chain immunostaining, whereas differentiated myotubes demonstrated a clear increase of immunostaining for both proteins with an apparent correlation between the level of differentiation and intensity of immunostaining (Fig. 1*C*). In myotubes, myocilin staining was dispersed throughout the cytoplasm and was more intense at or near the cell membrane. This pattern of staining is different from the typical perinuclear staining pattern observed in many cell types, including trabecular meshwork cells.

This observation prompted us to check whether myocilin is secreted from myotubes. Analysis of cell lysates and conditioned medium demonstrated that myocilin is not efficiently secreted from myotubes. Other secretory proteins (*e.g.* pigment epithelium-derived factor) were easily detected in the conditioned medium (Fig. 1*D*), indicating that the general secretory

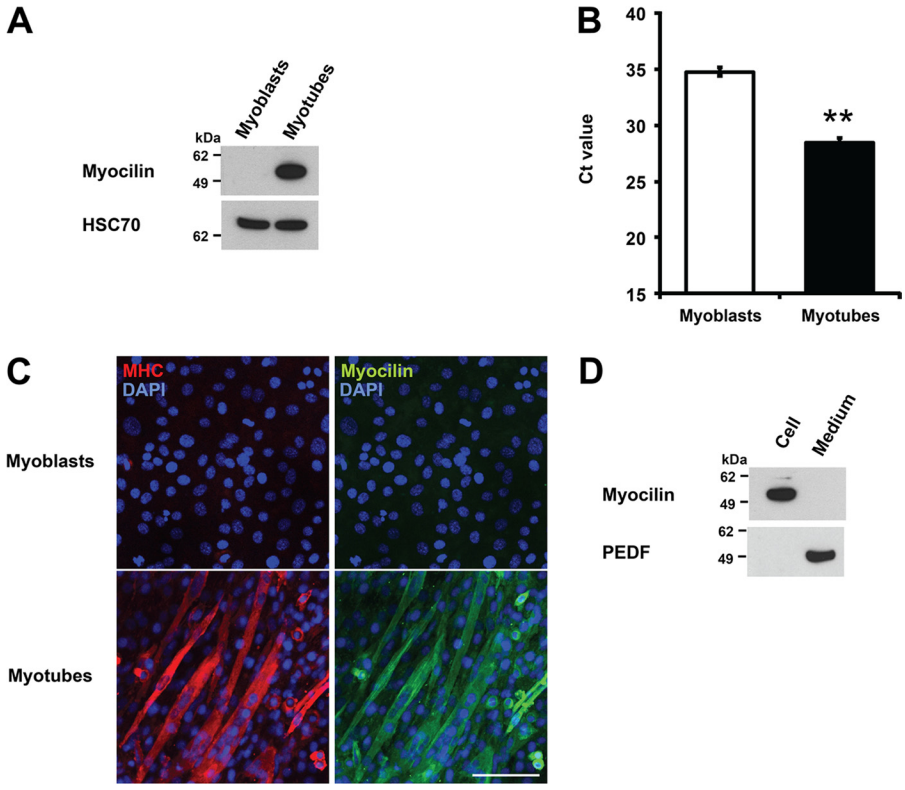

FIGURE 1. **Myocilin expression in differentiating C2C12 cells.** *A*, Western blot analysis of myocilin expression in undifferentiated myoblasts (day 0) and differentiating myotubes (day 5). Equal amounts of lysates were probed with antibodies against myocilin (1:4000 dilution) and HSC70 (1:2000 dilution). *B*, relative abundance of *Myoc* mRNA in mouse myoblasts (day 0) and myotubes (day 5) ($n = 3$ each) was evaluated on the basis of *Ct* values obtained by real-time PCR. Normalization was performed using GAPDH mRNA. *Error bars*, S.E. **, $p < 0.01$. *C*, myoblasts (day 0) and myotubes (day 5) were stained with antibodies against myosin heavy chain (*MHC*; 1:100 dilution) and myocilin (1:100 dilution) as described under "Experimental Procedures." *Scale bar*, 100 μm. *D*, myocilin is not efficiently secreted from myotubes. C2C12 myoblasts were differentiated for 5 days and maintained in serum-free medium for an additional 5 days. The lysate and conditioned medium were probed with anti-myocilin antibodies (1:4000 dilution) and anti-pigment epithelium-derived factor antibodies (*PEDF*; 1:5000 dilution).

pathway is intact in C2C12 myotubes. Altogether, these data suggest that myocilin is an intracellular protein in muscle cells and may interact with cytoplasmic proteins in these cells.

Myocilin Interacts with α1-Syntrophin, Cytoplasmic Component of Dystrophin-associated Protein Complex, in Muscle Tissues—To identify proteins interacting with myocilin, we performed yeast two-hybrid screening using a human skeletal muscle cDNA library and myocilin (positions 33–504) with its signal peptide deleted as a bait (23). Among 24 selected positive clones, one clone was identified by sequence analysis as a clone containing partial α1-Syn sequence (GenBank™ accession number U40571; positions 308–505). α1-Syn is a component of DAPC. Because it has been reported that another component of DAPC, β-dystrobrevin, may interact with olfactomedin 1, a protein related to myocilin (24), we decided to study the potential interaction between myocilin and α1-Syn in more details. To identify myocilin regions interacting with α1-Syn in yeast, we used an α1-Syn prey construct and myocilin bait constructs containing full-length myocilin, the N-terminal coiled-coil-containing region (positions 33–245) and the C-terminal olfactomedin domain-containing region (positions 246–504). Growth on selective medium (−AHLT) indicates the presence of an interaction between a bait and a prey. Full-length myocilin and the N-terminal region of myocilin constructs interacted with α1-Syn, whereas the C-terminal myocilin construct did not interact with α1-Syn in yeast (Fig. 2*A*).

DAPC complex consists of several cytoplasmic proteins, an extracellular protein, and two transmembrane protein complexes (25–27). Defects in the function and assembly of DAPC may lead to muscular dystrophies that in many cases have cognitive and neuropsychiatric components (25). Five different syntrophins have been reported in mammals, and they were named α1-, β1-, β2-, γ1-, and γ2-syntrophin (28). α1-Syn was shown to be the predominant syntrophin type in skeletal and cardiac muscles (29, 30), and its level dramatically increases in differentiating C2C12 myotubes (31). To confirm that myocilin may interact with syntrophins in mammalian cells in physiological conditions, we performed co-immunoprecipitation experiments using C2C12 myotubes and skeletal muscles. Antibodies against myocilin immunoprecipitated syntrophins, and antibody against pan-syntrophin immunoprecipitated myocilin from lysates of C2C12 myotubes and skeletal muscles (Fig. 2, *B* and *C*).

Intracellular localization of myocilin and α1-Syn confirmed their possible interaction. In differentiated C2C12 myotubes, myocilin immunostaining was preferentially observed at or close to the cell membrane, where it overlapped with that for α1-Syn (Fig. 3, *top row*). Weaker myocilin staining was also dispersed over the cytoplasm, where it overlapped with that for myosin heavy chain (Fig. 3, *bottom row*). On the basis of these results, we concluded that myocilin can interact with a cytoplasmic DAPC-associated protein, α1-Syn, in skeletal muscles.

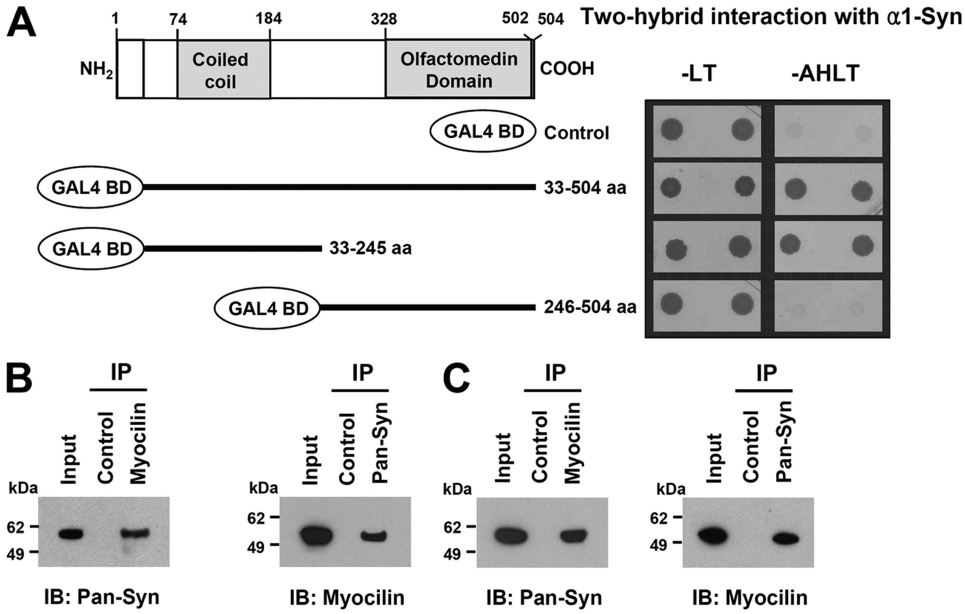

FIGURE 2. **Interaction of myocilin and α1-syntrophin in yeast and mammalian cells.** *A*, yeasts co-expressing α1-Syn and the indicated myocilin fusion proteins were spotted on −LT medium to confirm mating and on −AHLT medium to confirm protein-protein interactions between bait and prey proteins. *B* and *C*, lysates of C2C12 myotubes (*B*) or skeletal muscles (*C*) were immunoprecipitated with antibodies against myocilin or pan-syntrophin. Immunoprecipitates were collected, separated by SDS-PAGE, and then probed with HRP-conjugated pan-syntrophin antibodies or myocilin antibodies. Rabbit or mouse IgG was used as a control. Input lanes contained 5% of lysates used for immunoprecipitation. *aa*, amino acids; *IP*, immunoprecipitation; *IB*, immunoblot.

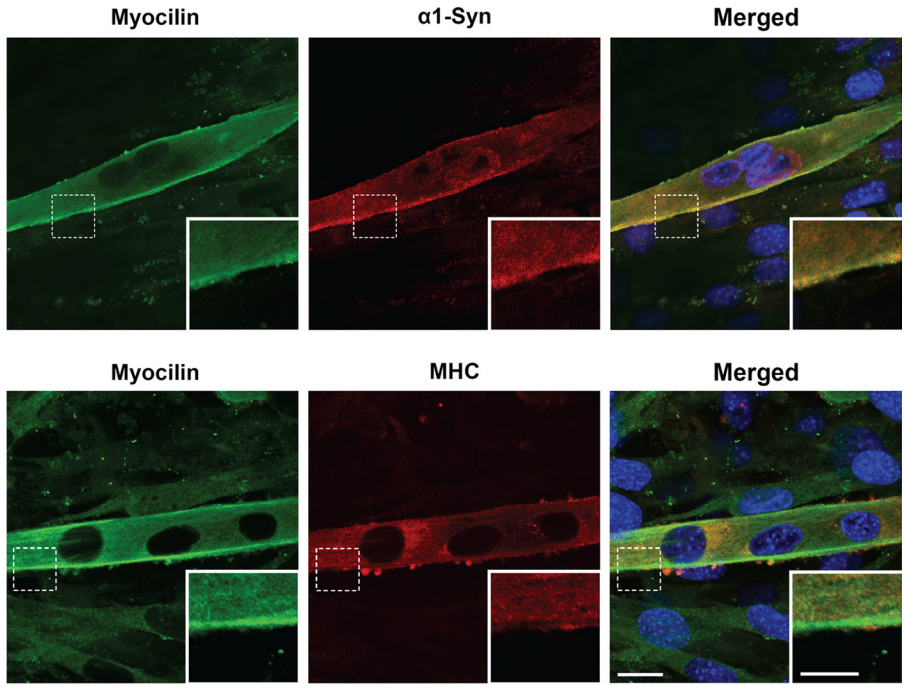

FIGURE 3. **Co-localization of myocilin and α1-syntrophin at the membrane of C2C12 myotubes.** C2C12 myotubes were stained with antibodies against α1-Syn and myocilin (*top row*) or myosin heavy chain (*MHC*) and myocilin (*bottom row*). The *inset* in the *bottom right corner* of each image shows the higher magnification for the area surrounded by the *dotted line*. The *yellow color* in *merged panels* represents co-localization. *Scale bar*, 20 μm; *scale bar* in *inset*, 10 μm.

Overexpression of Myocilin in Vivo Leads to Intracellular Redistribution of DAPC Proteins—α1-Syn is a cytosolic adaptor of DAPC involved in anchoring cell signaling molecules to the plasma membrane and in DAPC-mediated cell signaling (32). Myocilin interaction with the α1-Syn suggests that myocilin may play a role in the assembly and signaling through DAPC. To test this hypothesis, we analyzed the components of DAPC in the skeletal muscles of myocilin-overexpressing transgenic mice and wild-type mice. The transgenic mice were previously produced using bacterial artificial chromosome DNA containing the full-length mouse *Myoc* gene and long flanking sequences (33). Control experiments showed that the myocilin levels increased in the skeletal muscles between 2 and 12 months of age and declined in 24-month-old mice (supplemental Fig. 1). Most of the subsequent experiments were performed with males that were between 7 and 9 months old. Similar to the

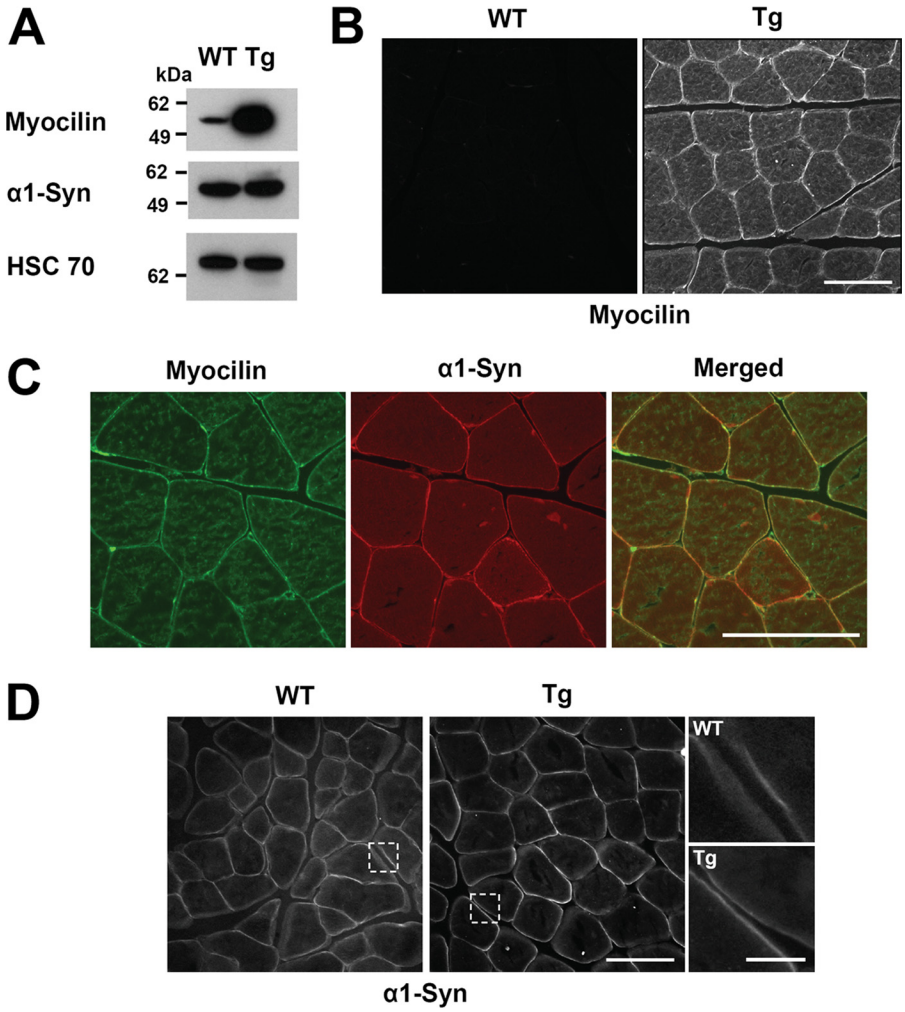

FIGURE 4. **Overexpression of myocilin *in vivo* induces relocalization of α1-syntrophin.** *A*, total muscle lysates were prepared from 8-month-old wild-type and transgenic (*Tg*) mice. Equal amounts of muscle lysates were probed with antibodies against myocilin (1:4000 dilution), α1-Syn (1:2000 dilution), and HSC70 (1:2000 dilution). *B*, myocilin immunofluorescence was performed using 10 μM frozen sections of the TA muscles from 8-month-old wild-type and transgenic mice. *C*, frozen sections of TA muscle from transgenic mice was double-stained with antibodies against myocilin and α1-Syn. The *merged green* and *red signals* indicate their co-localization at the sarcolemma. *D*, α1-Syn immunofluorescence was performed on frozen cross-sections as in *B*. Higher magnification of the areas surrounded by *dotted lines* is shown to the *right*. *Scale bar*, 100 μm; *scale bar* in *right-hand raw images* in *D*, 20 μm.

eye angle tissues, both myocilin mRNA and protein levels were 15-fold higher in skeletal muscles of adult transgenic mice as compared with wild-type littermates as judged by real-time PCR (not shown) and Western blotting (Fig. 4*A*). Immunostaining of skeletal muscle sections also showed a dramatic increase in the intensity of myocilin staining in the skeletal muscle of transgenic mice *versus* wild-type littermates. Myocilin signals were very low in the muscle of wild-type mice, but they were clearly detected around the sarcolemma and sarcoplasm of the transgenic line (Fig. 4*B*). Double immunostaining for myocilin and syntrophin revealed their co-localization at the sarcolemma of skeletal muscle of adult transgenic mice (Fig. 4*C*). These staining results are compatible with those of the differentiated myotubes shown in Fig. 3.

The levels of α1-Syn were similar in the skeletal muscles of wild-type and transgenic mice as judged by Western blotting (Fig. 4*A*). However, α1-Syn was redistributed in the muscles of transgenic mice compared with wild-type mice and was associated mainly with the sarcolemma (Fig. 4*D*), where it was co-localized with myocilin (Fig. 4*C*). Higher magnification images clearly showed that α1-Syn concentration was higher at the sarcolemma of transgenic mouse compared with wild-type littermates (Fig. 4*D*). Next, we compared the levels of different protein components of DAPC in the skeletal muscles of wild-type and transgenic animals after lysis of muscle tissues in a buffer containing 15% SDS. The levels of all tested DAPC components appeared to be similar in the muscles of 8-month-old transgenic and wild-type animals. However, the quantification showed a minor elevation of dystrophin level in the muscles of transgenic animals compared with wild-type littermates (Fig. 5*A*).

Myocilin could be precipitated from lysates of muscle tissues with antibodies against dystrophin (Fig. 5*B*) or β-DG (not shown). When mild lysis conditions were used (1% Igepal CA-630-containing buffer), similar levels of dystrophin were detected in the input and precipitated lanes of wild-type and transgenic muscles (Fig. 5*B*). However, significantly higher amounts of myocilin, α1-Syn, and nNOS were immunoprecipitated with dystrophin from transgenic as compared with wild-type muscle tissues (Fig. 5*B*). Analysis of skeletal muscles of

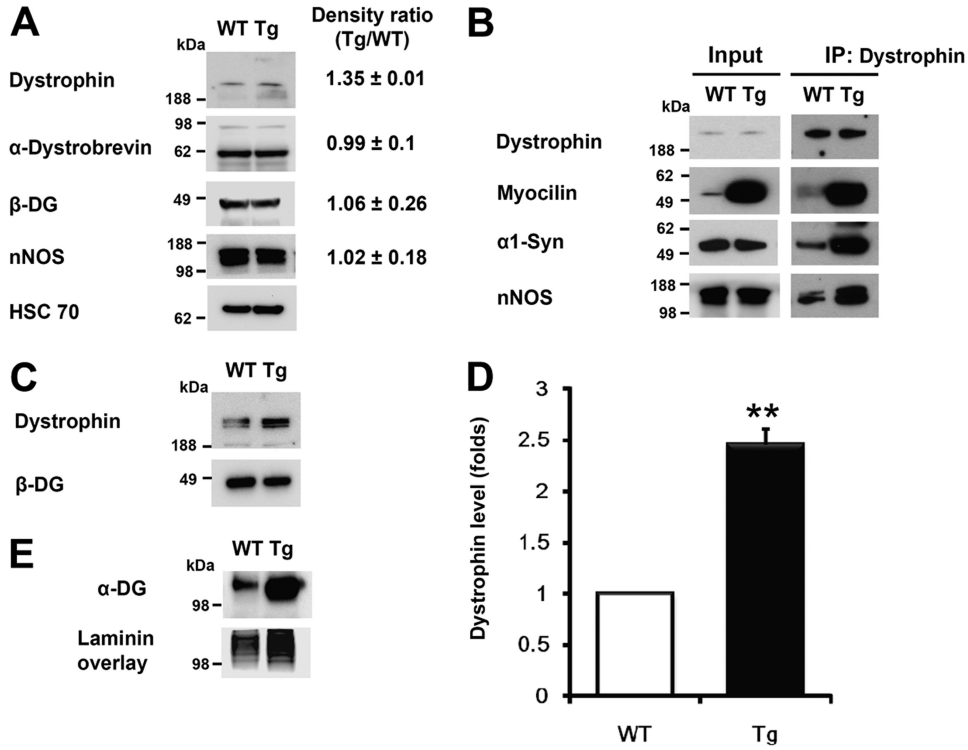

FIGURE 5. **Overexpression of myocilin *in vivo* induces relocalization of DAPC components to dystrophin and the binding of α-DG to laminin.** *A*, total muscle lysates prepared from 8-month-old wild-type and transgenic (*Tg*) mice were probed with antibodies against dystrophin (1:20 dilution), α-dystrobrevin (1:1000 dilution), β-DG (1:1000 dilution), nNOS (1:1000 dilution), and HSC70 (1:2000 dilution). Density ratios were calculated from two independent experiments using the ImageJ program. *B*, the indicated muscle lysates were immunoprecipitated with antibodies against dystrophin. Immunoprecipitates were probed with antibodies against dystrophin (1:20 dilution), myocilin (1:4000 dilution), α1-Syn (1:4000 dilution), and nNOS (1:1000 dilution). *C*, WGA elutes from digitonin-solubilized muscle lysates were probed with antibodies against dystrophin (1:20 dilution) and β-DG (1:1000 dilution). *D*, quantification of the results shown in *C*. Levels of dystrophin were normalized relative to β-DG levels from three independent experiments using the ImageJ program. *Error bars*, S.E. **, $p < 0.01$. *E*, WGA elutes were probed with α-DG (IIH6; 1:500 dilution) and further analyzed by a laminin overlay assay.

myocilin null mice demonstrated that the absence of myocilin led to a moderate reduction in the amount of syntrophin associated with dystrophin compared with wild-type littermates (supplemental Fig. 2). These results suggested that association of myocilin with DAPC may lead to a redistribution of some DAPC-associated proteins.

Published data indicated that the syntrophin-dystrobrevin complex serves as a linker between dystrophin and membrane-spanning complex and is important for DAPC stability (34, 35). Because elevated levels of myocilin increased the association of α1-Syn with dystrophin (Fig. 5*B*), we hypothesized that this may increase the association of dystrophin with transmembrane proteins and contribute to the stabilization of the DAPC. To prove this hypothesis, we compared the biochemical stability of dystrophin-dystroglycan interaction using a technique described previously (35). We assessed the levels of dystrophin in the WGA glycoprotein-enriched elutes containing a high concentration of dystroglycans and their associated proteins. The dystrophin level was increased by 2.5-fold in the WGA elutes of transgenic mouse skeletal muscle compared with wild-type littermates (Fig. 5, *C* and *D*). Increased stability of DAPC may increase the level of functional α-DG at the sarcolemma. To test the level of functional α-DG, we used the IIH6 antibody that recognizes the functional glycan epitope of α-DG that is necessary for laminin binding. The level of the active form of α-DG was markedly increased in the muscle of transgenic mice as compared with wild-type littermates (Fig. 5*E*). A significant increase of laminin-α-DG binding was also observed in the muscle of transgenic mice compared with wild-type littermates using a laminin overlay assay (Fig. 5*E*). Increased binding of laminin to α-DG may stimulate laminin-regulated signaling pathways.

Changes of Muscle Atrophy and Hypertrophy Pathways in Myocilin-transgenic Mice—Previous studies have shown that binding of laminin to the α-DG receptor can activate Akt signaling (36, 37). Phospho-Akt was clearly increased in C2C12 myotubes growing on laminin-coated plates compared with non-coated plates, suggesting that laminin-stimulated activation of Akt signaling occurs in myotubes (Fig. 6*A*). A high level of myocilin increased laminin-α-DG binding in the muscle of transgenic mice (Fig. 5*E*); this could also activate Akt signaling in myocilin-rich muscle. Akt is a pivotal molecule that mediates muscle hypertrophy and inhibits muscle atrophy (38). FoxO3a is a transcription factor that can be phosphorylated by Akt (39, 40). In the case of muscle atrophy, FoxO3a is dephosphorylated and transported into the nucleus to up-regulate atrophy-related genes (40). It has also been reported that FoxO3a may be activated by nitric oxide that is produced by nNOS dislocated from DAPC (41). Above, we showed that although the total levels of nNOS were similar, the levels of dystrophin-associated nNOS were clearly increased in the muscle tissues of transgenic as compared with wild-type mice, implying that levels of dissociated nNOS were reduced (Fig. 5, *A* and *B*). In addition, the levels of phospho-Akt and phospho-FoxO3a were increased by

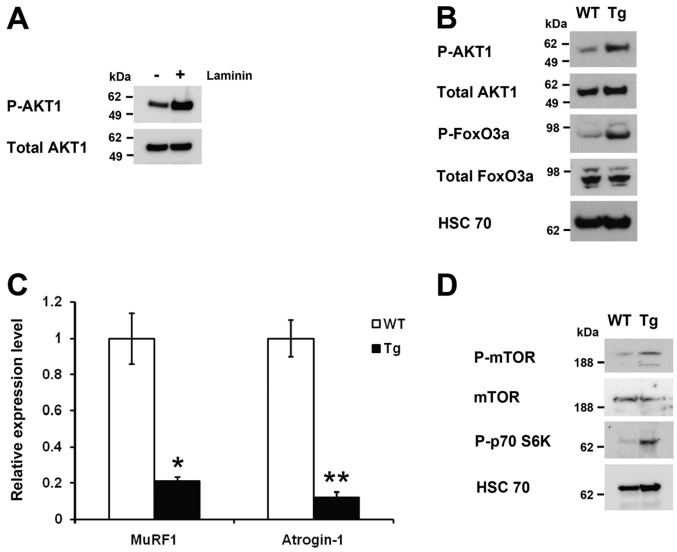

FIGURE 6. **Changes in muscle hypertrophy and atrophy signaling pathways in myocilin expressing transgenic mouse.** *A*, total lysates from C2C12 myotubes differentiated on the plates with or without laminin were probed with antibodies against phospho-AKT1 (*P-AKT1*; 1:1000 dilution) and total AKT1 (1:2000 dilution). *B*, total muscle lysates were prepared from 8-month-old wild-type and transgenic (*Tg*) mice. Equivalent amounts of muscle lysates were separated by SDS-PAGE and then probed with antibodies against phospho-AKT1 (1:1000 dilution), total AKT1 (1:2000 dilution), phospho-FoxO3a (1:1000 dilution), FoxO3a (1:1000 dilution), and HSC70 (1:2000 dilution). *C*, mRNA levels of MuRF-1 and atrogin-1 in the muscles of 8-month-old wild-type and transgenic mice ($n = 3$) were quantified by real-time PCR. *Error bars*, S.E. *, $p < 0.05$; **, $p < 0.01$. *D*, total muscle lysates as in *B* were probed with antibodies against phospho-mTOR (*P-mTOR*; 1:500 dilution), total mTOR (1:500 dilution), phospho-p70^{S6K} (1:500 dilution), and HSC70 (1:2000 dilution).

3.2- and 3.5-fold, respectively, in the muscles of 8-month-old transgenic mice as compared with wild-type animals (Fig. 6*B*). We concluded that both increased Akt activity and reduced levels of dissociated nNOS could contribute to increased levels of phosphorylated FoxO in the muscles of transgenic mice. FoxO3a induces expression of the ubiquitin ligases MuRF-1 and atrogin-1 (42). Their up-regulation can promote muscle cell degradation through the ubiquitin proteasome pathway during the muscle atrophy process (43). The levels of MuRF-1 and atrogin-1 were decreased by 79 and 88%, respectively, in the muscles of transgenic mice compared with wild-type animals (Fig. 6*C*). We concluded that down-regulation of MuRF-1 and atrogin-1 may contribute to the prevention of muscle atrophy in the transgenic mice. Additionally, Akt can control the skeletal muscle hypertrophy pathway by regulating mTOR pathway and its downstream target p70^{S6K} (44). The phospho-mTOR and p70^{S6K} were increased in the muscle of transgenic mice compared with wild-type littermates (Fig. 6*D*). Decreased levels of phospho-Akt were observed in the muscle of myocilin null mice (supplemental Fig. 2), supporting the idea that myocilin may be involved in the regulation of Akt signaling. Muscular atrophy and hypertrophy signaling pathways are tightly regulated, and the changes in these pathways can change the size of skeletal muscles (38). We hypothesized that myocilin may be involved in the regulation of fiber size of skeletal muscle through the hypertrophy and atrophy signaling pathways.

Overexpression of Myocilin Leads to Muscle Hypertrophy in Transgenic Mice—Examination of the skeletal muscles of wild-type and transgenic mice after skin removal demonstrated increased skeletal muscle mass in the legs of transgenic mice compared with those of control mice (Fig. 7*A*). To quantify this observation, we dissected and weighed one of the largest and prominent muscles of the hind limb, the gastrocnemius muscle. The average weight of the gastrocnemius muscle increased more than 40% in transgenic mice compared with that of wild-type littermates (Fig. 7*B*). To determine whether the increase in skeletal muscle mass of transgenic mice resulted from muscular hypertrophy, we stained the cross-sections of TA muscles with H&E and Masson's trichrome (Fig. 7*C*). Muscle fibers of transgenic mice had a normal polygonal shape and peripheral nuclei, although the cross-sectional areas of entire fibers appeared to be enlarged compared with that of wild-type mice. No pathological alterations, such as central nuclei, excessive fibrous tissues, and rounded fibers, were observed in the muscles of transgenic mice (Fig. 7*C*). The enlargement of muscle fibers in transgenic mice most probably is not due to the pseudohypertrophic muscular dystrophy. Staining with the antibody against laminin, a major component of the basal lamina surrounding muscle fibers (45), clearly showed the boundaries of muscle fibers. Analysis of the stained cross-sections also revealed that the muscle fiber size of transgenic mice was increased compared with that of wild-type mice (Fig. 7*D*). The ratio of small fibers with a size of $<2000\ \mu m^2$ was remarkably decreased, whereas the ratio of large size fibers ($>2000\ \mu m^2$) was increased in transgenic mice as compared with wild-type mice (Fig. 7*E*). The average size of the fibers was increased by 36.4% in transgenic mice compared with control mice (Fig. 7*F*). Although we did not carefully examine the fiber size of other muscles beyond TA muscle, we found that similar levels of myocilin and phospho-Akt were present in three different hind limb muscles, TA, gastrocnemius, and quadricep muscles (supplemental Fig. 3). These results suggest that myocilin may work similarly in various parts of skeletal muscles. We concluded that overexpression of myocilin in skeletal muscles leads to muscle fiber hypertrophy, and this may contribute to the increase in skeletal muscle mass of transgenic mice as compared with wild-type mice.

DISCUSSION

Glaucoma-causing mutations in the *MYOC* gene were first identified more than 10 years ago (8, 10). Since then, the potential for myocilin to be used as a molecular tool to study glaucoma has stimulated active investigation into the function(s) of myocilin protein. However, despite these efforts, the role of myocilin in ocular and non-ocular tissues remains elusive. There is a growing number of cases showing that mutations in interacting proteins may produce similar phenotypes and that protein-protein interactions may be used to identify new candidate genes for diseases (46). Therefore, multiple attempts have been made to identify proteins that interact with myocilin and several candidate proteins belonging to different functional classes (extracellular matrix, cytoskeleton, cell signaling and metabolism, and membrane proteins) have been identified (5, 6, 23, 47). In many cases, interaction of myocilin with other

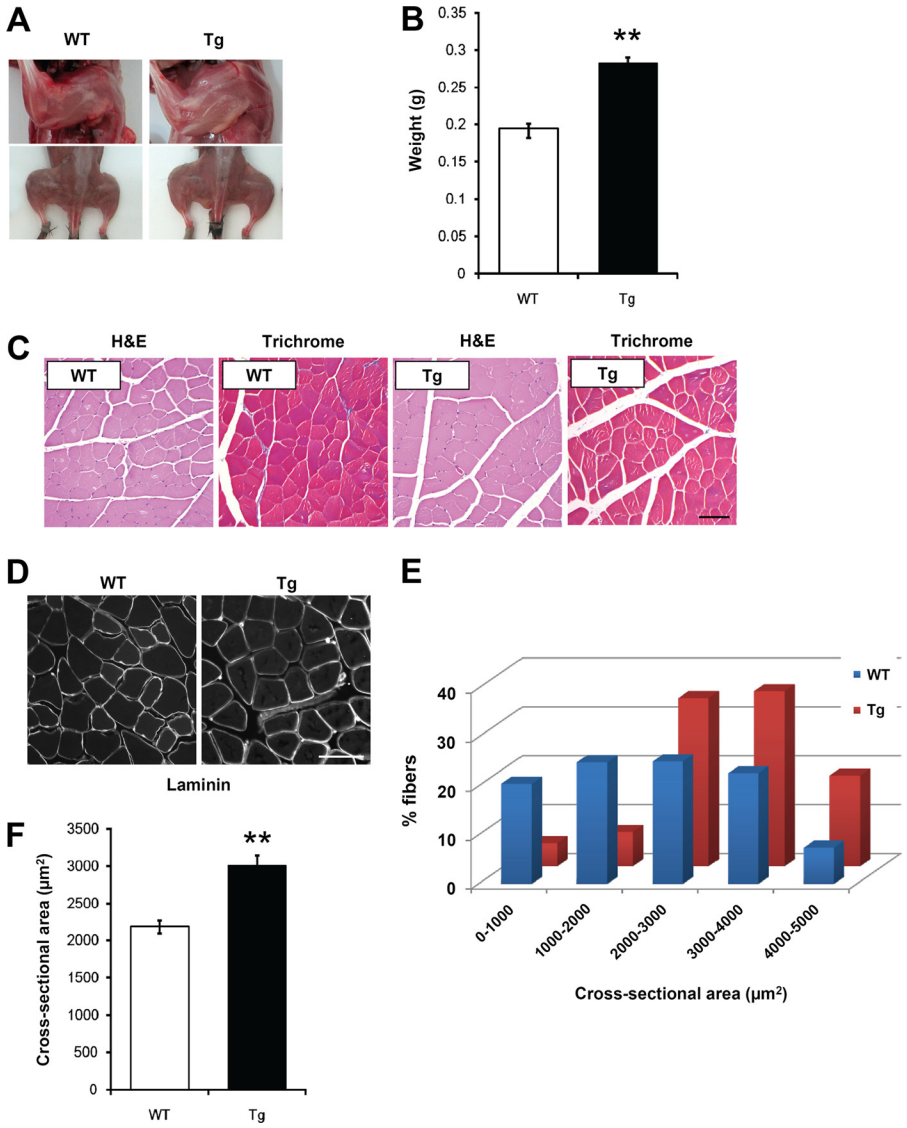

FIGURE 7. **Increased skeletal muscle mass in myocilin-expressing transgenic mice compared with wild-type mice.** *A*, increased skeletal muscle mass in legs of transgenic (*Tg*) mice compared with that of control mice. *B*, increased weight of dissected gastrocnemius muscles in transgenic mice. *C*, H&E and Masson's trichrome staining of TA muscle cross-sections (10 μm). *Scale bar*, 100 μm. *D*, laminin immunofluorescence of frozen cross-sections (10 μm) of TA muscles from 8-month-old wild-type and transgenic littermates; *scale bar*, 100 μm. *E*, cross-sectional area of muscle fibers stained with laminin in *D* was measured using ImageJ (National Institutes of Health). Size distribution of fibers was plotted as a percentage of total fiber number. *F*, average fiber size was determined from five independent pairs of mice according to the same analysis as in *E*. *Error bars*, S.E. **, $p < 0.01$.

proteins could not be confirmed by independent techniques (47), and continuing work should be undertaken to confirm the specificity of these interactions. Using independent techniques, including a yeast two-hybrid assay and co-immunoprecipitation from cultured cells and native tissues, we demonstrate here that myocilin interacts with α1-Syn. Our preliminary data indicate that in other tissues, myocilin may also interact with β-syntrophin.[3] At first glance, an interaction between secretory (myocilin) and cytoplasmic (syntrophin) proteins seems unusual. However, accumulating evidence demonstrates that many signal peptide-containing proteins may have distinct functions outside of the secretory pathway. For example, endoplasmic reticulum-resident protein calreticulin was identified as a binding protein to the cytoplasmic α-subunits of integrin receptors (48), the DNA-binding domain of a nuclear receptor (49), and p21 mRNA (50) through independent studies. Alternative cellular localizations would provide functional diversity from a single protein through the interaction with different molecules that are present at the different cellular compartments. Data presented here suggest that myocilin is not secreted from muscle cells. The absence of myocilin secretion is not a unique property of muscle cells; myocilin is also not secreted from trabecular meshwork cells growing in culture in the presence of different concentrations of serum (51) and the human breast adenocarcinoma MCF7 cell line (52). NIH3T3 cells transfected with myocilin constructs do not secret myocilin, whereas transfected HEK293 and COS7 cells efficiently secret myocilin in the same conditions (14). Published results indicate that suppression of myocilin secretion does not dramatically affect general secretion *in vivo* and *in vitro* (14, 52, 53).

[3] M. K. Joe and S. I. Tomarev, unpublished observations.

Myocilin may have a distinct function in the cytoplasm that is different from its functions in the extracellular space.

Syntrophins share a similar domain organization and functional conservation among the isotypes. The syntrophins interact with various components of the DAPC and bind to the C-terminal region of dystrophin (26, 28, 30). α1-Syn is a cytoplasmic component of the DAPC that serves as a scaffolding adapter. The PDZ domain of α1-Syn binds to several membrane proteins, including nNOS, sodium channels, kinases, and aquaporin 4 (25, 26). The PDZ domain of α1-Syn most probably is not essential for interactions with myocilin because this domain was absent in the yeast clone identified by an yeast two-hybrid screen and because myocilin and the C-terminal region of α1-Syn without the PDZ domain were co-localized well in mammalian cells transfected with corresponding constructs.[3] The N-terminal domain of myocilin (without the olfactomedin domain) is essential for interaction with α1-Syn (Fig. 2).

It has been shown that expression of α1-Syn and its binding to the components of DAPC may be modified in myofibers from patients with common forms of muscle dystrophies (54, 55). It has been suggested that changes in the recruitment of α1-Syn to the sarcolemma might lead to a disturbance of intracellular signaling and affect muscle function (55). Overexpression of myocilin in the muscles of transgenic mice also led to a redistribution of some DAPC-associated proteins, including syntrophin, and may have affected intracellular signaling. Oppositely, the absence of myocilin led to a moderate reduction in the amount of syntrophin associated with dystrophin and reduced levels of phospho-Akt in the muscle of myocilin null mice compared with wild-type littermates.

We demonstrated that overexpression of myocilin in skeletal muscles led to muscle hypertrophy. Skeletal muscle hypertrophy results from an increase in the diameter of muscle fibers that are formed after the differentiation and fusion of myoblast precursors. Several signaling pathways have been implicated in muscle hypertrophy, including the insulin-like growth factor 1/phosphoinositide/Akt signaling pathway, which contributes to regulation of skeletal muscle fiber size (56). Activation of this cascade keeps the FoxO3 transcription factor in an inactive (phosphorylated) state and sequesters FoxO3 in the cytosol (40). Activation of FoxO3 stimulates transcription of a number of genes, including atrophy-linked ubiquitin ligases astrogin-1 and MuRF-1 (40). Recent data demonstrate that transcription factor JunB is important for the maintenance of adult muscle size and can induce rapid hypertrophy and block atrophy (57). However, although JunB blocks FoxO3 binding to atrogin-1 and MuRF-1 promoters, it induces hypertrophy independently of the Akt signaling pathway (57). We found that myocilin-induced muscle hypertrophy involves activation of the Akt signaling pathway and in this respect is more similar to insulin-like growth factor-1-induced skeletal myotube hypertrophy (56). Extracellular myocilin may serve as a modulator of Wnt signaling (22) and possess an ability to activate the integrin-FAK-PI3K-Akt signaling pathway (58). Because myocilin is not secreted from muscle cells, we believe that activation of the Akt signaling pathway in transgenic mice occurs mainly through the action of intracellular myocilin. One function of DAPC is to provide a connection between extracellular matrix and intracellular signaling. An elevated level of DAPC-associated myocilin leads to a redistribution of DAPC components that may stabilize DAPC and lead to enhanced binding of extracellular ligands, such as laminin, to DAPC (see Fig. 5). This in turn leads to the activation of Akt and phosphorylation of FoxO3a. Extracellular myocilin probably does not play a prominent role in skeletal muscles, although we cannot completely exclude participation of extracellular myocilin in the observed effects.

The mean cross-section area of muscle fibers was increased by 36% in myocilin transgenic mice compared with their wild-type littermates (Fig. 7*D*). This number is similar to that observed for mouse muscle fibers overexpressing JunB for 9 days (about 40% increase) (57). It has been suggested that the JunB increase can cause marked hypertrophy and can block the rapid loss of muscle mass in bed-ridden patients (57). Although more research is necessary, we speculate that increasing myocilin levels in skeletal muscle may also be considered as a potential new therapeutic approach to combat the muscle loss during certain diseases or in the elderly. Although myocilin was discovered as a gene that is up-regulated in the trabecular meshwork as a result of glucocorticoid treatment, myocilin was not identified among genes induced in skeletal muscles by the dexamethasone treatment (59–61). In skeletal muscles, dexamethasone treatment changed the expression pattern of hundreds of genes and could cause muscle atrophy (see Refs. 62 and 63 for recent reviews). In transgenic mice, myocilin overexpression is due to the increased copy number of the *Myoc* gene. Up-regulation of myocilin in the absence of glucocorticoid increase leads to changes that are opposite to those observed after glucocorticoid treatment at both molecular (down-regulation of MuRF1 and astrogin-1 *versus* their up-regulation) and tissue levels (muscle hypertrophy *versus* atrophy).

Experiments reported in this paper were performed using skeletal muscles because of the relative abundance of biological material for biochemical testing. Myocilin is highly expressed in the tissues of the eye angle, including the trabecular meshwork, sclera, iris, and ciliary muscle (5, 64). The state of ciliary muscle and its contractility are important for the architecture of the conventional trabecular meshwork outflow pathway and unconventional uveoscleral outflow pathway (65, 66). Modulations of these outflow pathways may lead to changes in intraocular pressure.

In summary, myocilin interacts with α1-Syn and co-immunoprecipitates with several DAPC components, including dystrophin and dystroglycan. Overexpression of myocilin in transgenic mice leads to redistribution of several DAPC components and increased phosphorylation of Akt, a key regulator of muscle size. Accordingly, muscle size was increased in transgenic mice compared with wild-type mice. We suggest that myocilin is a regulator of muscle hypertrophy/atrophy pathways and that the stabilization of DAPC and increased interaction with laminin may contribute to this regulation. Future studies will be aimed at elucidating the roles of myocilin and DAPC in the eye drainage structures to determine how the elevated levels of myocilin may change the DAPC complex in these structures and whether overexpression of myocilin affects contractility of the ciliary muscle.

Acknowledgments—We thank Dr. Heung Sun Kwon for myocilin constructs and Dr. Thomas V. Johnson and Nicholas Dekorver for critical reading of the manuscript.

REFERENCES

1. Polansky, J. R., Fauss, D. J., Chen, P., Chen, H., Lütjen-Drecoll, E., Johnson, D., Kurtz, R. M., Ma, Z. D., Bloom, E., and Nguyen, T. D. (1997) Cellular pharmacology and molecular biology of the trabecular meshwork inducible glucocorticoid response gene product. *Ophthalmologica* **211,** 126–139
2. Tomarev, S. I., and Nakaya, N. (2009) Olfactomedin domain-containing proteins. Possible mechanisms of action and functions in normal development and pathology. *Mol. Neurobiol.* **40,** 122–138
3. Nguyen, T. D., Chen, P., Huang, W. D., Chen, H., Johnson, D., and Polansky, J. R. (1998) Gene structure and properties of TIGR, an olfactomedin-related glycoprotein cloned from glucocorticoid-induced trabecular meshwork cells. *J. Biol. Chem.* **273,** 6341–6350
4. Fautsch, M. P., and Johnson, D. H. (2001) Characterization of myocilin-myocilin interactions. *Invest. Ophthalmol. Vis. Sci.* **42,** 2324–2331
5. Torrado, M., Trivedi, R., Zinovieva, R., Karavanova, I., and Tomarev, S. I. (2002) Optimedin. A novel olfactomedin-related protein that interacts with myocilin. *Hum. Mol. Genet.* **11,** 1291–1301
6. Wentz-Hunter, K., Ueda, J., and Yue, B. Y. (2002) Protein interactions with myocilin. *Invest. Ophthalmol. Vis. Sci.* **43,** 176–182
7. Fingert, J. H., Ying, L., Swiderski, R. E., Nystuen, A. M., Arbour, N. C., Alward, W. L., Sheffield, V. C., and Stone, E. M. (1998) Characterization and comparison of the human and mouse *GLC1A* glaucoma genes. *Genome Res.* **8,** 377–384
8. Stone, E. M., Fingert, J. H., Alward, W. L., Nguyen, T. D., Polansky, J. R., Sunden, S. L., Nishimura, D., Clark, A. F., Nystuen, A., Nichols, B. E., Mackey, D. A., Ritch, R., Kalenak, J. W., Craven, E. R., and Sheffield, V. C. (1997) Identification of a gene that causes primary open angle glaucoma. *Science* **275,** 668–670
9. Kwon, Y. H., Fingert, J. H., Kuehn, M. H., and Alward, W. L. (2009) Primary open-angle glaucoma. *N. Engl. J. Med.* **360,** 1113–1124
10. Adam, M. F., Belmouden, A., Binisti, P., Brézin, A. P., Valtot, F., Béchetoille, A., Dascotte, J. C., Copin, B., Gomez, L., Chaventré, A., Bach, J. F., and Garchon, H. J. (1997) Recurrent mutations in a single exon encoding the evolutionarily conserved olfactomedin homology domain of TIGR in familial open-angle glaucoma. *Hum. Mol. Genet.* **6,** 2091–2097
11. Quigley, H. A., and Broman, A. T. (2006) The number of people with glaucoma worldwide in 2010 and 2020. *Br. J. Ophthalmol.* **90,** 262–267
12. Jacobson, N., Andrews, M., Shepard, A. R., Nishimura, D., Searby, C., Fingert, J. H., Hageman, G., Mullins, R., Davidson, B. L., Kwon, Y. H., Alward, W. L., Stone, E. M., Clark, A. F., and Sheffield, V. C. (2001) Non-secretion of mutant proteins of the glaucoma gene myocilin in cultured trabecular meshwork cells and in aqueous humor. *Hum. Mol. Genet.* **10,** 117–125
13. Gobeil, S., Rodrigue, M. A., Moisan, S., Nguyen, T. D., Polansky, J. R., Morissette, J., and Raymond, V. (2004) Intracellular sequestration of hetero-oligomers formed by wild-type and glaucoma-causing myocilin mutants. *Invest. Ophthalmol. Vis. Sci.* **45,** 3560–3567
14. Malyukova, I., Lee, H. S., Fariss, R. N., and Tomarev, S. I. (2006) Mutated mouse and human myocilins have similar properties and do not block general secretory pathway. *Invest. Ophthalmol. Vis. Sci.* **47,** 206–212
15. Sohn, S., Hur, W., Joe, M. K., Kim, J. H., Lee, Z. W., Ha, K. S., and Kee, C. (2002) Expression of wild-type and truncated myocilins in trabecular meshwork cells. Their subcellular localizations and cytotoxicities. *Invest. Ophthalmol. Vis. Sci.* **43,** 3680–3685
16. Joe, M. K., Sohn, S., Hur, W., Moon, Y., Choi, Y. R., and Kee, C. (2003) Accumulation of mutant myocilins in ER leads to ER stress and potential cytotoxicity in human trabecular meshwork cells. *Biochem. Biophys. Res. Commun.* **312,** 592–600
17. Liu, Y., and Vollrath, D. (2004) Reversal of mutant myocilin non-secretion and cell killing. Implications for glaucoma. *Hum. Mol. Genet.* **13,** 1193–1204
18. Joe, M. K., and Tomarev, S. I. (2010) Expression of myocilin mutants sensitizes cells to oxidative stress-induced apoptosis. Implication for glaucoma pathogenesis. *Am. J. Pathol.* **176,** 2880–2890
19. Tomarev, S. I., Tamm, E. R., and Chang, B. (1998) Characterization of the mouse *Myoc*/*Tigr* gene. *Biochem. Biophys. Res. Commun.* **245,** 887–893
20. Kim, B. S., Savinova, O. V., Reedy, M. V., Martin, J., Lun, Y., Gan, L., Smith, R. S., Tomarev, S. I., John, S. W., and Johnson, R. L. (2001) Targeted disruption of the myocilin gene (*Myoc*) suggests that human glaucoma-causing mutations are gain of function. *Mol. Cell. Biol.* **21,** 7707–7713
21. Lam, D. S., Leung, Y. F., Chua, J. K., Baum, L., Fan, D. S., Choy, K. W., and Pang, C. P. (2000) Truncations in the TIGR gene in individuals with and without primary open-angle glaucoma. *Invest. Ophthalmol. Vis. Sci.* **41,** 1386–1391
22. Kwon, H. S., Lee, H. S., Ji, Y., Rubin, J. S., and Tomarev, S. I. (2009) Myocilin is a modulator of Wnt signaling. *Mol. Cell. Biol.* **29,** 2139–2154
23. Joe, M. K., Sohn, S., Choi, Y. R., Park, H., and Kee, C. (2005) Identification of flotillin-1 as a protein interacting with myocilin. Implications for the pathogenesis of primary open-angle glaucoma. *Biochem. Biophys. Res. Commun.* **336,** 1201–1206
24. Veroni, C., Grasso, M., Macchia, G., Ramoni, C., Ceccarini, M., Petrucci, T. C., and Macioce, P. (2007) β-Dystrobrevin, a kinesin-binding receptor, interacts with the extracellular matrix components pancortins. *J. Neurosci. Res.* **85,** 2631–2639
25. Waite, A., Tinsley, C. L., Locke, M., and Blake, D. J. (2009) The neurobiology of the dystrophin-associated glycoprotein complex. *Ann. Med.* **41,** 344–359
26. Ehmsen, J., Poon, E., and Davies, K. (2002) The dystrophin-associated protein complex. *J. Cell Sci.* **115,** 2801–2803
27. Hynes, R. O., and Zhao, Q. (2000) The evolution of cell adhesion. *J. Cell Biol.* **150,** F89–F96
28. Piluso, G., Mirabella, M., Ricci, E., Belsito, A., Abbondanza, C., Servidei, S., Puca, A. A., Tonali, P., Puca, G. A., and Nigro, V. (2000) γ1- and γ2-syntrophins, two novel dystrophin-binding proteins localized in neuronal cells. *J. Biol. Chem.* **275,** 15851–15860
29. Peters, M. F., Adams, M. E., and Froehner, S. C. (1997) Differential association of syntrophin pairs with the dystrophin complex. *J. Cell Biol.* **138,** 81–93
30. Ahn, A. H., Freener, C. A., Gussoni, E., Yoshida, M., Ozawa, E., and Kunkel, L. M. (1996) The three human syntrophin genes are expressed in diverse tissues, have distinct chromosomal locations, and each bind to dystrophin and its relatives. *J. Biol. Chem.* **271,** 2724–2730
31. Kim, M. J., Hwang, S. H., Lim, J. A., Froehner, S. C., Adams, M. E., and Kim, H. S. (2010) A-syntrophin modulates myogenin expression in differentiating myoblasts. *PLoS ONE* **5,** e15355
32. Ervasti, J. M., and Sonnemann, K. J. (2008) Biology of the striated muscle dystrophin-glycoprotein complex. *Int. Rev. Cytol.* **265,** 191–225
33. Gould, D. B., Miceli-Libby, L., Savinova, O. V., Torrado, M., Tomarev, S. I., Smith, R. S., and John, S. W. (2004) Genetically increasing Myoc expression supports a necessary pathologic role of abnormal proteins in glaucoma. *Mol. Cell. Biol.* **24,** 9019–9025
34. Yoshida, M., Hama, H., Ishikawa-Sakurai, M., Imamura, M., Mizuno, Y., Araishi, K., Wakabayashi-Takai, E., Noguchi, S., Sasaoka, T., and Ozawa, E. (2000) Biochemical evidence for association of dystrobrevin with the sarcoglycan-sarcospan complex as a basis for understanding sarcoglycanopathy. *Hum. Mol. Genet.* **9,** 1033–1040
35. Bunnell, T. M., Jaeger, M. A., Fitzsimons, D. P., Prins, K. W., and Ervasti, J. M. (2008) Destabilization of the dystrophin-glycoprotein complex without functional deficits in α-dystrobrevin null muscle. *PLoS ONE* **3,** e2604
36. Xiong, Y., Zhou, Y., and Jarrett, H. W. (2009) Dystrophin glycoprotein complex-associated Gβγ subunits activate phosphatidylinositol 3-kinase/Akt signaling in skeletal muscle in a laminin-dependent manner. *J. Cell. Physiol.* **219,** 402–414
37. Langenbach, K. J., and Rando, T. A. (2002) Inhibition of dystroglycan binding to laminin disrupts the PI3K/AKT pathway and survival signaling in muscle cells. *Muscle Nerve* **26,** 644–653
38. Sandri, M. (2008) Signaling in muscle atrophy and hypertrophy. *Physiology* **23,** 160–170
39. Glass, D. J. (2005) A signaling role for dystrophin. Inhibiting skeletal mus-

cle atrophy pathways. *Cancer Cell* **8,** 351–352
40. Sandri, M., Sandri, C., Gilbert, A., Skurk, C., Calabria, E., Picard, A., Walsh, K., Schiaffino, S., Lecker, S. H., and Goldberg, A. L. (2004) Foxo transcription factors induce the atrophy-related ubiquitin ligase atrogin-1 and cause skeletal muscle atrophy. *Cell* **117,** 399–412
41. Suzuki, N., Motohashi, N., Uezumi, A., Fukada, S., Yoshimura, T., Itoyama, Y., Aoki, M., Miyagoe-Suzuki, Y., and Takeda, S. (2007) NO production results in suspension-induced muscle atrophy through dislocation of neuronal NOS. *J. Clin. Invest.* **117,** 2468–2476
42. Senf, S. M., Dodd, S. L., McClung, J. M., and Judge, A. R. (2008) Hsp70 overexpression inhibits NF-κB and Foxo3a transcriptional activities and prevents skeletal muscle atrophy. *FASEB J.* **22,** 3836–3845
43. Bodine, S. C., Latres, E., Baumhueter, S., Lai, V. K., Nunez, L., Clarke, B. A., Poueymirou, W. T., Panaro, F. J., Na, E., Dharmarajan, K., Pan, Z. Q., Valenzuela, D. M., DeChiara, T. M., Stitt, T. N., Yancopoulos, G. D., and Glass, D. J. (2001) Identification of ubiquitin ligases required for skeletal muscle atrophy. *Science* **294,** 1704–1708
44. Bodine, S. C., Stitt, T. N., Gonzalez, M., Kline, W. O., Stover, G. L., Bauerlein, R., Zlotchenko, E., Scrimgeour, A., Lawrence, J. C., Glass, D. J., and Yancopoulos, G. D. (2001) Akt/mTOR pathway is a crucial regulator of skeletal muscle hypertrophy and can prevent muscle atrophy *in vivo*. *Nat. Cell Biol.* **3,** 1014–1019
45. Gullberg, D., Tiger, C. F., and Velling, T. (1999) Laminins during muscle development and in muscular dystrophies. *Cell. Mol. Life Sci.* **56,** 442–460
46. Oti, M., Snel, B., Huynen, M. A., and Brunner, H. G. (2006) Predicting disease genes using protein-protein interactions. *J. Med. Genet.* **43,** 691–698
47. Fautsch, M. P., Vrabel, A. M., and Johnson, D. H. (2006) The identification of myocilin-associated proteins in the human trabecular meshwork. *Exp. Eye Res.* **82,** 1046–1052
48. Leung-Hagesteijn, C. Y., Milankov, K., Michalak, M., Wilkins, J., and Dedhar, S. (1994) Cell attachment to extracellular matrix substrates is inhibited upon down-regulation of expression of calreticulin, an intracellular integrin α-subunit-binding protein. *J. Cell Sci.* **107,** 589–600
49. Burns, K., Duggan, B., Atkinson, E. A., Famulski, K. S., Nemer, M., Bleackley, R. C., and Michalak, M. (1994) Modulation of gene expression by calreticulin binding to the glucocorticoid receptor. *Nature* **367,** 476–480
50. Iakova, P., Wang, G. L., Timchenko, L., Michalak, M., Pereira-Smith, O. M., Smith, J. R., and Timchenko, N. A. (2004) Competition of CUGBP1 and calreticulin for the regulation of p21 translation determines cell fate. *EMBO J.* **23,** 406–417
51. Resch, Z. T., Hann, C. R., Cook, K. A., and Fautsch, M. P. (2010) Aqueous humor rapidly stimulates myocilin secretion from human trabecular meshwork cells. *Exp. Eye Res.* **91,** 901–908
52. Hardy, K. M., Hoffman, E. A., Gonzalez, P., McKay, B. S., and Stamer, W. D. (2005) Extracellular trafficking of myocilin in human trabecular meshwork cells. *J. Biol. Chem.* **280,** 28917–28926
53. Zhou, Y., Grinchuk, O., and Tomarev, S. I. (2008) Transgenic mice expressing the Tyr437His mutant of human myocilin protein develop glaucoma. *Invest. Ophthalmol. Vis. Sci.* **49,** 1932–1939
54. Wakayama, Y., Inoue, M., Kojima, H., Jimi, T., Yamashita, S., Kumagai, T., Shibuya, S., Hara, H., and Oniki, H. (2006) Altered α1-syntrophin expression in myofibers with Duchenne and Fukuyama muscular dystrophies. *Histol. Histopathol.* **21,** 23–34
55. Nakamori, M., Kimura, T., Kubota, T., Matsumura, T., Sumi, H., Fujimura, H., Takahashi, M. P., and Sakoda, S. (2008) Aberrantly spliced α-dystrobrevin alters α-syntrophin binding in myotonic dystrophy type 1. *Neurology* **70,** 677–685
56. Rommel, C., Bodine, S. C., Clarke, B. A., Rossman, R., Nunez, L., Stitt, T. N., Yancopoulos, G. D., and Glass, D. J. (2001) Mediation of IGF-1-induced skeletal myotube hypertrophy by PI3K/Akt/mTOR and PI3K/Akt/GSK3 pathways. *Nat. Cell Biol.* **3,** 1009–1013
57. Raffaello, A., Milan, G., Masiero, E., Carnio, S., Lee, D., Lanfranchi, G., Goldberg, A. L., and Sandri, M. (2010) JunB transcription factor maintains skeletal muscle mass and promotes hypertrophy. *J. Cell Biol.* **191,** 101–113
58. Kwon, H. S., and Tomarev, S. I. (2011) Myocilin, a glaucoma-associated protein, promotes cell migration through activation of integrin-focal adhesion kinase-serine/threonine kinase signaling pathway. *J. Cell. Physiol.* **226,** 3392–3402
59. Wu, Y., Zhao, W., Zhao, J., Zhang, Y., Qin, W., Pan, J., Bauman, W. A., Blitzer, R. D., and Cardozo, C. (2010) REDD1 is a major target of testosterone action in preventing dexamethasone-induced muscle loss. *Endocrinology* **151,** 1050–1059
60. Carraro, L., Ferraresso, S., Cardazzo, B., Romualdi, C., Montesissa, C., Gottardo, F., Patarnello, T., Castagnaro, M., and Bargelloni, L. (2009) Expression profiling of skeletal muscle in young bulls treated with steroidal growth promoters. *Physiol. Genomics* **38,** 138–148
61. Komamura, K., Shirotani-Ikejima, H., Tatsumi, R., Tsujita-Kuroda, Y., Kitakaze, M., Miyatake, K., Sunagawa, K., and Miyata, T. (2003) Differential gene expression in the rat skeletal and heart muscle in glucocorticoid-induced myopathy. Analysis by microarray. *Cardiovasc. Drugs Ther.* **17,** 303–310
62. Schakman, O., Gilson, H., and Thissen, J. P. (2008) Mechanisms of glucocorticoid-induced myopathy. *J. Endocrinol.* **197,** 1–10
63. Hasselgren, P. O., Alamdari, N., Aversa, Z., Gonnella, P., Smith, I. J., and Tizio, S. (2010) Corticosteroids and muscle wasting. Role of transcription factors, nuclear cofactors, and hyperacetylation. *Curr. Opin. Clin. Nutr. Metab. Care* **13,** 423–428
64. Senatorov, V., Malyukova, I., Fariss, R., Wawrousek, E. F., Swaminathan, S., Sharan, S. K., and Tomarev, S. (2006) Expression of mutated mouse myocilin induces open-angle glaucoma in transgenic mice. *J. Neurosci.* **26,** 11903–11914
65. Tamm, E. R. (2009) The trabecular meshwork outflow pathways. Structural and functional aspects. *Exp. Eye Res.* **88,** 648–655
66. Alm, A., and Nilsson, S. F. (2009) Uveoscleral outflow. A review. *Exp. Eye Res.* **88,** 760–768